Optical properties of Ge and Si nanocrystallites from *ab initio* calculations. I. Embedded nanocrystallites

H.-Ch. Weissker, J. Furthmüller, and F. Bechstedt
Institut für Festkörpertheorie und Theoretische Optik, Friedrich-Schiller-Universität, 07743 Jena, Germany
(Received 31 July 2001; revised manuscript received 7 December 2001; published 11 April 2002)

We present parameter-free calculations of the frequency-dependent dielectric function in order to understand the optical properties of Ge and Si nanoparticles embedded in a crystalline matrix. The calculations are based upon the independent-particle approximation and a pseudopotential-plane-wave method. The nanoparticles are modeled by clusters of up to 239 atoms embedded in cubic SiC as a host material with a wide energy gap. The dependence of the resulting optical spectra on the nanocrystallite size, the crystallite-host interface, and the crystallite-crystallite interaction is studied.

DOI: 10.1103/PhysRevB.65.155327 PACS number(s): 78.66.Db, 73.22.−f, 73.21.−b

I. INTRODUCTION

The physics of nanoparticles presents particularly interesting aspects, mainly related to the strong modifications of the fundamental properties of the material due to the spatial confinement in three dimensions. Remarkable effects on the joint density of states, on the optical absorption and luminescence spectra, and on the nonlinear optical behavior have been either predicted or observed. Until now, in the case of Ge and Si nanocrystals the efforts have been concentrated on the study of the fundamental band gap.[1–7] Nanometer-sized Si and Ge structures give rise to an efficient photoluminescence (PL) in the visible, including even the blue or violet, wavelength region. Recently it has also been discovered that nanocrystalline (nc) Si and Ge materials shows PL in the red and near-infrared spectral region depending on the nanoscale size.[2,7] Such nanostructures have been fabricated by ion implantation in SiO_2 matrices,[8,9] cosputtering,[7] thermal evaporization in a buffer gas,[3,10] or by Stranski-Krastanov growth on crystalline substrates.[5,6,11]

The origin of the photoluminescence has been investigated for different systems by many authors. Quantum-confined excitons give rise to strongly size-dependent emission.[7] Luminescence from surface or interface states exhibits only little size dependence. While there is necessarily a breakdown of the **k**-conservation rule due to the spatial confinement, it is by no means clear how this will affect the oscillator strengths, in particular, the transition probabilities of the transitions near the absorption edge, of nanocrystallites made of indirect-band-gap semiconductors. Research has to answer the question[6,12] of whether the localization results in strong transitions at or close to the highest occupied molecular orbital–lowest unoccupied molecular orbital gap.

Apart from the optical properties near the fundamental gap, the group-IV semiconductors treated in this work also possess higher optical transitions with rather large oscillator strengths. For example, the most important E_1 (E_2) transitions in bulk Ge occur around 2.2 (4.5) eV, well above the indirect and direct (E_0) band gaps with energies of 0.6 and 0.9 eV, respectively.[13] For Si crystals the corresponding values are 1.1 (indirect), 4.2 (E_0), 3.5 (E_1), and 4.3 (E_2) eV.[13] There have been only few experimental studies of the modification of these high-energy transitions in nanocrystalline materials. They involve optical absorption and resonant Raman spectroscopy.[8,10,14] The size dependence of the high-energy transitions is not known in detail and, hence, not understood. So far, only quantum-confinement effects on the fundamental band gap in nanocrystalline systems have been explained theoretically.[15–18] However, there is still a controversy about the correct treatment of the many-body effects in the calculation of the electron-hole pair excitation energies.[17–21]

There have been very few theoretical studies of the higher optical transitions. There are calculations of optical spectra of nc Si using the empirical-pseudopotential approach[22] or the tight-binding (TB) method,[23] the transferability of which to a nanocrystalline material is questionable. Only very recently, *ab initio* spectra have been published.[24] For Ge nanocrystallites, TB spectra have been calculated recently.[25,26]

In this paper we study the optical properties of Ge and Si nanocrystallites in a wide spectral range from first principles in the framework of the independent-particle approximation. Since embedded and free nanocrystals behave completely different with respect to their electronic and optical properties, we present the results for the two classes of nanocrystalline materials in two successive papers. In part I, the optical properties of strained Ge and Si nanocrystals embedded in a crystalline matrix are studied. Cubic silicon carbide (SiC) is taken as the host material. On the one hand, it represents a wide-band-gap semiconductor. On the other hand, it is not clear if, and how, the lowest-energy transitions of the nanocrystals fit into its fundamental gap. In the forthcoming part II of the paper we discuss the properties of free Ge and Si nanocrystallites, the surface bonds of which are saturated by hydrogen. In this way we model very high barriers at the crystallite-host interfaces.

The present part I of the paper is organized as follows. In Sec. II we present the electronic-structure method and discuss the difficulties in the calculation of the frequency-dependent dielectric function. Spherical Ge and Si nanocrystallites embedded in SiC are studied in Sec. III. The results are discussed in the light of the underlying electronic structure. Finally, in Sec. IV we give a brief summary.

 ©2002 The American Physical Society

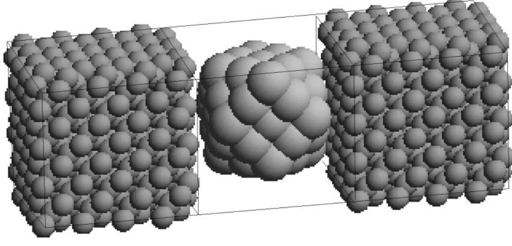

FIG. 1. Three adjacent simple-cubic supercells of 512 atoms. The inclusion of the 83-atom nanocrystal is shown. In the central supercell, the host material is not displayed.

II. COMPUTATIONAL METHODS

A. Electronic structure of nanocrystals

In a first step we calculate the one-electron states from first principles using the density-functional theory[27] (DFT) in the local-density approximation (LDA).[28] The electron-electron interaction is described within the parametrization of Perdew and Zunger.[29] Nonlinear core corrections are taken into account.[30] The interaction of the electrons with the atomic cores is treated by non-norm-conserving *ab initio* Vanderbilt pseudopotentials.[31] They allow a substantial potential softening even for first-row elements.[32] For instance, in the SiC case the plane-wave expansion of the eigenfunctions is restricted by a cutoff of 13.2 Ry. We use the VIENNA *ab initio* SIMULATION PACKAGE.[33] The DFT-LDA yields cubic lattice constants of $a_0=4.332$, 5.398, 5.627 Å and indirect fundamental energy gaps $E_g=1.33$, 0.46, 0.00 eV for unstrained SiC, Si, and Ge, respectively.

The plane-wave expansion requires a supercell approach to the description of nanocrystallites or quantum dots. We consider an arrangement of simple-cubic (sc) cells. The use of the soft Vanderbilt pseudopotentials[32] allows to treat extremely large supercells with 512 atoms in the case of a tetrahedrally coordinated bulk. Their edge length amounts to 1.75 nm in the cubic-SiC case. This length increases to 2.26 nm in the case of pure Ge. For the purpose of comparison and to study the effect of the interaction between the nanocrystallites we also consider smaller sc supercells with 216 or 64 atoms. In order to model embedded spherical nanocrystallites we replace host material atoms in the center of the supercell by Ge or Si atoms as schematically indicated in Fig. 1. Thereby we start from one atom and consecutively replace the respective following shells of next neighbors. The atomic structure remains unchanged, i.e., the atoms keep tetrahedral coordination, and all bonds in the interface between the nanocrystallite and the host are saturated. The crystallites possess nearly spherical symmetry. The point group of the supercell system is still T_d. The resulting nanocrystals of 1, 5, 17, 41, 83, 147, and 239 atoms are highly strained due to the large lattice misfit between Ge, or Si, and SiC. The Ge crystallites possess different interface bonds Ge-Si or Ge-C, depending on the choice of a Si or C site as the center of the nanocrystal. Moreover, the numbers of Si and C atoms constituting the host material are different. The size of the nanostructures is limited by that of the supercell, but also for physical reasons. Such highly strained systems cannot occur above a critical diameter. Moreover, the strained Ge tends to become a semimetal, at least within DFT-LDA.

In the forthcoming paper, part II, we study hydrogenated (nearly) spherical crystallites with tetrahedrally coordinated Ge or Si atoms as shown in Fig. 1 but at bulk atomic distances. The hydrogen passivation with the huge energetical splitting between the antibonding and bonding Ge-H or Si-H states simulates high barriers for both electrons and holes in the nanocrystal. Apart from the fact that these nanostructures represent free crystallites with passivated surfaces, they may also be regarded as models for unstrained nanocrystals embedded in a semiconductor matrix with a fundamental energy gap larger than that of cubic SiC, e.g., hexagonal SiC, or in a matrix of a crystalline or amorphous insulator, e.g., SiO_2 or sapphire.

B. Optical properties of supercell arrangements

The optical properties of an ordered arrangement of nanocrystallites are evaluated within the independent-particle approximation and using the Bloch representation of the artificial supercell crystal.[34] The imaginary part of the dielectric function ($\alpha=x,y,z$)

$$\operatorname{Im}\varepsilon_{\alpha\alpha}(\omega)=\frac{(2\pi e\hbar)^2}{m\Omega_0}\frac{1}{N}\sum_{\mathbf{k}}\sum_{c,v}\frac{f_{cv}^{\alpha\alpha}(\mathbf{k})}{\varepsilon_c(\mathbf{k})-\varepsilon_v(\mathbf{k})}\delta(\varepsilon_c(\mathbf{k})-\varepsilon_v(\mathbf{k})-\hbar\omega), \tag{1}$$

$$f_{cv}^{\alpha\alpha}(\mathbf{k})=\frac{2m|\langle c\mathbf{k}|v_\alpha|v\mathbf{k}\rangle|^2}{\varepsilon_c(\mathbf{k})-\varepsilon_v(\mathbf{k})} \tag{2}$$

contains optical transitions between valence- ($|v\mathbf{k}\rangle$) and conduction- ($|c\mathbf{k}\rangle$) band states with the oscillator strengths $f_{cv}^{\alpha\alpha}(\mathbf{k})$ taken at N $\mathbf{k}$ points in the Brillouin zone (BZ). Ω_0 is the volume of the supercell. Interestingly, the luminescence intensity is related to the absorption coefficient through an energy balance relation as long as the structure of the nanocrystallites is not changed in the excited state.[35,36] The absorption is directly linked to the imaginary part of the dielectric function (1). When quasiparticle effects describing the excitation behavior[37] are included in the computation, the energies in the Dirac δ function have to be shifted.[34] In principle, one has to solve simultaneously the Bethe-Salpeter equation to account for the electron-hole interaction.[38] Delerue *et al.*[18] observed in TB calculations that the self-energy effects and Coulomb corrections almost cancel each other for nanocrystallites being not too small and not too large. This can be taken as a further justification to start with the independent-particle approximation and LDA energies as a first step. For a detailed discussion of the fine structure in the optical spectra the inclusion of all the many-body effects is needed. However, for the discussion of the trends with the size, the surface chemistry, and the surroundings of the nanocrystals, the framework of the independent-particle approximation should be sufficient.[34]

One disadvantage of using pseudowave functions is related to the representation of the optical transition operator. The velocity operator **v** cannot be directly related to the momentum operator **p** because of the nonlocality of the

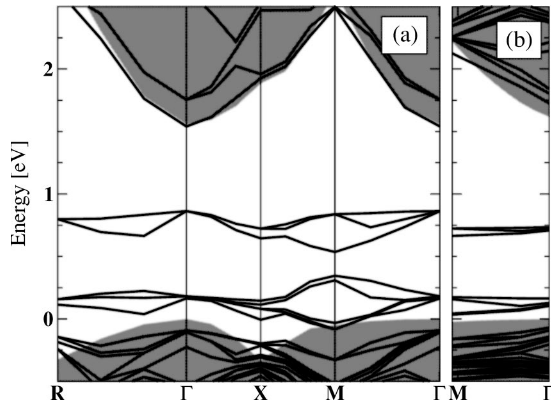

FIG. 2. (a) Band structure of the 41-atom Ge nanocrystal in a 216-atom cell, (b) that of the same nanocrystal in a 512-atom cell. The host material is cubic SiC, the crystallite-host interface is Ge-C. The folded bands of the pure host material, SiC, are represented by the shaded regions.

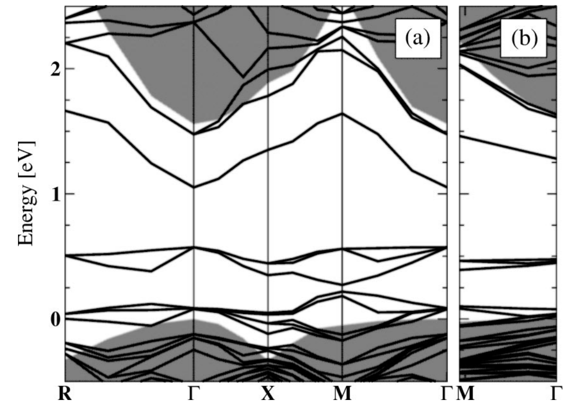

FIG. 3. (a) Band structure of the 41-atom Si nanocrystal in a 216-atom cell, (b) that of the same nanocrystal in a 512-atom cell. The host material is cubic SiC.

pseudopotentials.[34] This problem becomes even more complicated when the norm condition is lifted and non-norm-conserving ultrasoft pseudopotentials of the Vanderbilt type[31,32] are used. We resolve the accompanying uncertainty by applying Blöchl's projector-augmented wave (PAW) approach to the electronic-structure calculation.[39] There is a formal relationship between ultrasoft Vanderbilt-type pseudopotentials and the PAW method.[40] Using projectors onto the core regions of the free pseudoatoms, all-electron wave functions are constructed for the valence electrons.[41] As a consequence, a core-repair term[42] appears in the optical matrix elements. This approach gives indeed reasonable results for the optical properties of bulk semiconductors.[41]

The Brillouin-zone integration in Eq. (1) requires a **k**-point sampling density depending on the localization of electronic states and the supercell size. In the case of the hydrogenated crystallites the resulting bands are very flat and correspond to levels. One can restrict the computation to one **k** point in the BZ in connection with a Lorentzian broadening of the Dirac δ function. The real part of the dielectric function follows immediately using the principal value of the energy denominator corresponding to the δ function. In the case of the Ge and Si nanocrystallites embedded in cubic SiC the situation is different. All bands of the supercell arrangement are rather dispersive (cf. Fig. 2). However, their number and dispersion depend on both cluster and supercell size. Making use of the band dispersion we apply the linear tetrahedron method to the BZ integration over the δ function in expression (1) as well as for the single-particle density of states (DOS). A highly efficient integration scheme has been developed recently.[43] It allows the generation of the optical spectrum using the electronic structure at only one **k** point. The irreducible part of the simple-cubic BZ is itself a tetrahedron. Consequently the energies of the bands (or, more strictly speaking, band pairs c and v) are needed at the corners of the tetrahedron. Unfortunately, the multiple band crossings in the small BZ belonging to the 512-atom and 216-atom supercells may induce spurious singularities in the joint density of states.[44] In fact, it is impossible to allocate the energies at different **k** points to bands. These problems have been solved by using second-order $\mathbf{k}\cdot\mathbf{p}$ perturbation theory. All band energies and the interband and intraband momentum matrix elements are computed at one **k** point in the center of the tetrahedron. Since this point exhibits no spatial symmetry, degeneracies are avoided. The single tetrahedron is divided into many tetrahedra. The energies at all the vertices are taken from the $\mathbf{k}\cdot\mathbf{p}$ result. In the case of 512-atom supercells we typically divide the irreducible part of the BZ into 64 tetrahedra and use 2048 bands.

III. RESULTS AND DISCUSSION

A. Localized and extended states

The effect of the insertion of a nanocrystal into the SiC host material on the electronic structure is demonstrated in Figs. 2 and 3 for the 41-atom structures. For both group-IV materials, Ge or Si, nanocrystal-induced and, therefore, localized occupied states arise in the lower part of the energy gap of the host material. Due to the supercell description, these states are not really dispersionless. They show a behavior similar to that of the defect bands in supercell calculations. While exhibiting the highest degeneracy at the Γ point, they split even along the high-symmetry directions into several bands according to their s- or p-like orbital character. The main structures of the SiC DOS have been used for the alignment of the band structures.

Since the interaction between adjacent crystallites decreases with decreasing spatial separation, the crystallite-induced bands become more dispersive. A comparison of results obtained for 216-atom and 512-atom supercells in Figs. 2(a) and 2(b) shows that this is indeed the case. Evidently, the main features of the band structure close to the valence-band maximum (VBM) of SiC are the same for the 41-atom crystallite in the two different cells. This is a consequence of the strong Ge contributions to the corresponding wave functions, which are, therefore, rather localized. Comparing Figs. 2 and 3 we find that Ge and Si nanocrystallites behave differently in cubic SiC. For germanium, nanocrystallite-induced states only occur as occupied valence states in the lower part of the fundamental gap, not, however, as empty

conduction states closer to the conduction-band minimum of SiC. The situation is radically different for silicon. There are empty crystallite-induced bands within the host band gap. They exhibit a dispersion similar to that of the folded lowest conduction band of bulk SiC. Within a simple quantum-confinement model this result may be interpreted such that confined holes arise in both the Ge and the Si nanocrystals, while confinement of electrons takes place only in the latter system. Therefore, the system Ge in 3C-SiC is of a type-II heterostructure character,[45] whereas Si in 3C-SiC is of type I. However, due to the low barrier and the small sizes of the nanocrystallites and of the supercells, the localization is by no means complete. Sizable portions of the Si-related wave functions extend into the host material. The corresponding bands are dispersive, indicating that the crystallite-matrix system acts more as a composite material. The strong mixing of Si and SiC states induces the splitting and shift of conduction-band states into the fundamental gap. The observed heterostructure character is, in principle, in agreement with the results of Harrison's tight-binding model.[46] The conduction-band minima of the two materials give rise to a nearly flat band lineup.

While the distinction between the Ge crystallites with Ge-C crystallite-host interface on the one hand and of the Si crystallites on the other hand is clear cut, there seems to be some ambiguity when Ge crystallites with a Ge-Si crystallite-host interface are considered. For the 17-atom Ge crystallite with Ge-Si interface we found an unoccupied crystallite-induced band below the conduction-band minimum, appearing much like the similar band for the Si crystallites. We relate this result to the same atomic geometries. The interatomic distances in our model are those of cubic SiC, which means that both Si and Ge are highly compressively strained. This is also true for the interface bonds Ge-Si. Discussing this fact in terms of a tight-binding model[46] it seems natural that the equal coordination and the similar strain give rise to similar features. The interatomic matrix elements are identical. There is only a small variation in the intra-atomic terms of the tight-binding Hamiltonian.

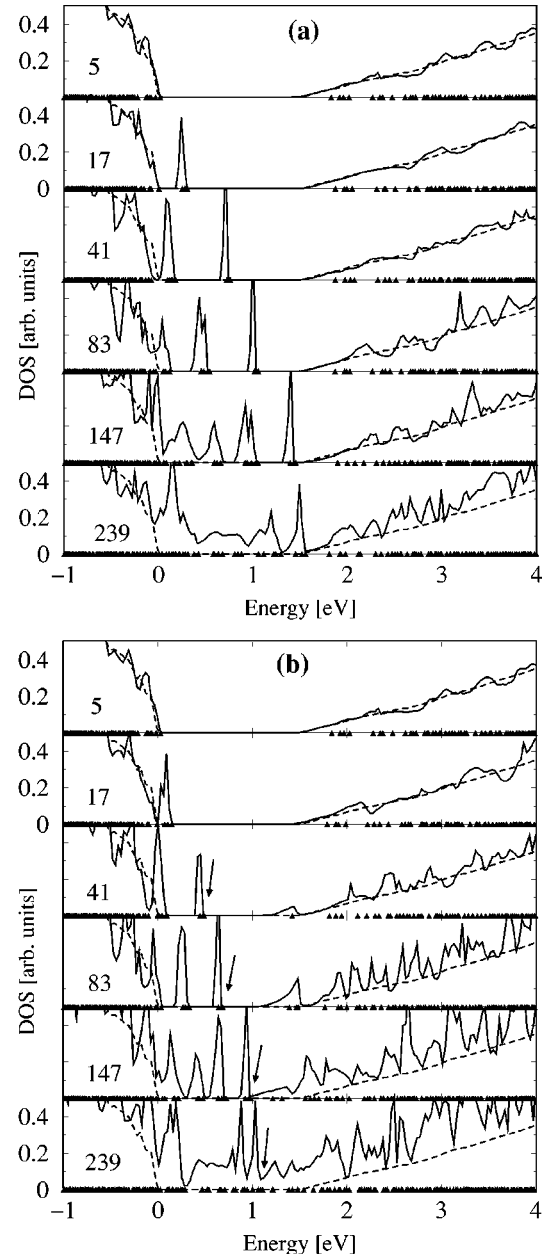

FIG. 4. Density of states for nanocrystals in SiC, as calculated in the 512-atom simple cubic cell. (a) Ge nanocrystals with Ge-C crystallite-host interfaces, (b) Si nanocrystals. Solid line, nanocrystal-host supercell system, dashed line, pure cubic SiC. The triangles indicate the electronic energies at the **k** point used in the electronic-stucture calculation. The arrows point to the highest occupied states. The energy zero is defined by the VBM of SiC.

B. Size effects

Looking at the electronic DOS one finds that the results for the 41-atom inclusions are representative for the other nanocrystallites that we have studied. The one-particle DOS for both Ge and Si crystallites in the 512-atom cells are plotted in Fig. 4. For comparison, the DOS of the pure host SiC is also shown. The main SiC-related peaks have been used for the energy alignment. The spectra depend on the number of atoms, which can be represented by a filling factor f, i.e., the ratio of the number of embedded atoms and the total number of atoms. Up to a crystallite size of 83 atoms, i.e., a filling factor of $f=0.162$, the DOS of the host material is conserved with regard to its main features. The ragged shape of the DOS indicates the transition from a system with extended states to one with partially localized states.

The DOS of Ge crystallites with a Ge-C interface are shown in Fig. 4(a). The Ge crystallites induce additional occupied states within the fundamental gap of the host close to its VBM. The number of these states increases with the crystallite size. Their positions shift to higher energies. This is in complete agreement with the prediction of a type-II heterostructure behavior. On the other hand, the DOS of the Si crystallites, presented in Fig. 4(b), shows unoccupied states near the conduction-band minimum, thereby verifying the type-I behavior. For the largest crystallites we have studied, those of 147 and 239 atoms representing filling factors of $f=0.287$ and $f=0.467$, the main bulk features of the host disappear, the gap is not clearly recognizable and is filled

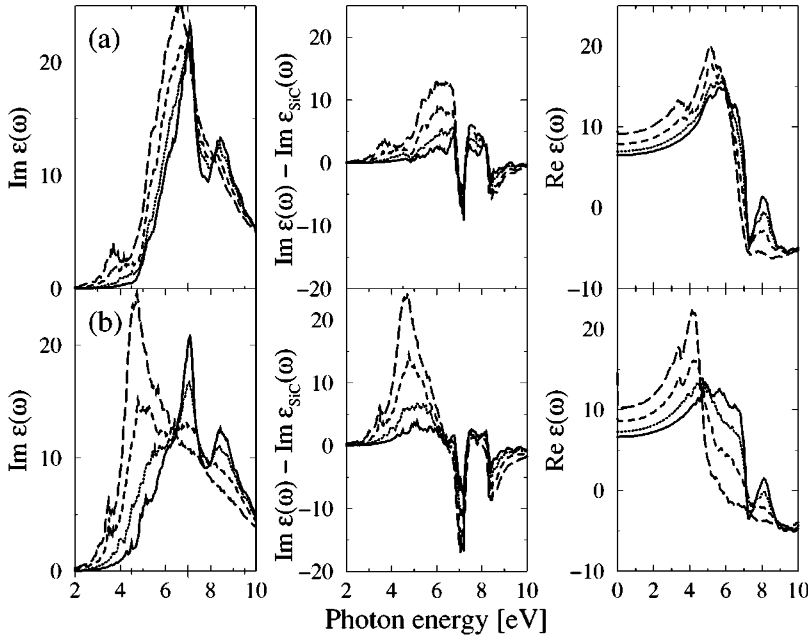

FIG. 5. Dielectric function $\varepsilon(\omega)$ of Ge embedded in cubic SiC with Ge-C crystallite-host interface (a), (b) Si nanocrystals. The imaginary part (left panels), the difference $\mathrm{Im}\,\varepsilon(\omega) - \mathrm{Im}\,\varepsilon_{SiC}(\omega)$ (middle panels), and the real part (right panels) are plotted. Solid line, 41-atom; dotted line, 83-atom, dashed line, 147-atom; long-dashed line, 239-atom crystallite.

with states, both occupied and unoccupied. Therefore it is not possible to draw simple comparisons between extended and localized states as in the case of the smaller crystallites. This is not surprising. For the large filling factors of the order of 0.5 it is clearly not a good approach to think of the crystallites as being embedded in some host material without changing its properties. Rather, the systems under consideration represent composite materials with an inhomogeneous distribution of the atomic species.

The findings of the band structure and DOS calculations enable us to understand the behavior of the dielectric function plotted in Fig. 5. We compare the imaginary and the real part of the dielectric function of Ge crystallites with a Ge-C interface to those of Si crystallites. In order to visualize the changes more clearly, the differences of the calculated spectra and the SiC spectrum are also shown. Again, the computations have been carried out for 512-atom cells. The real parts of the dielectric function are calculated from the imaginary parts by means of the Kramers-Kronig relations. They show a typical oscillator behavior with an additional high-energy feature. Therefore we focus our attention on the imaginary part.

With increasing size of the nanocrystallites there is a significant deviation from the spectra of the pure cubic SiC.[34] The high-energy SiC peak with mixed E_1', E_0', and $E_2+\delta$ character, located at about 9 eV in the DFT-LDA absorption spectrum, is strongly reduced. For the larger crystallites of 147 and 239 atoms it vanishes altogether. This is in agreement with the result that the DOS loses its clearly recognizable host bulk features for these filling factors. Despite the difference in their heterostructure behavior, the spectra of Ge and Si crystallites develop similarly with varying crystallite size. The difference spectra for both types show strong negative peaks at about 7 and 8.5 eV, which do not change their energetical position with increasing crystallite size. We attribute these peaks to the vanishing of the SiC bulk properties discussed above.

The lower-energy SiC peak at about 7 eV decreases and shifts to smaller photon energies. It does so more strongly for Si than for Ge. For the largest crystallites the absorption tends to become similar to results found for compressed Ge and Si. Comparing the shifts and the difference spectra for the Ge crystallites it can be seen that the main structure between about 5 and 8 eV is attributable to the increasing amount of crystallite material. Its shift seems to be unaffected by spatial confinement. In the difference spectrum this main structure between 5 and 8 eV is just cut slightly above 7 eV by the strong negative difference peak due to the vanishing SiC properties. The same explanation holds for the Si crystallites, except that now the main absorption structure lies at lower energies between 3.5 and 6 eV.

The most interesting part of the spectra lies below the main structures discussed above. Below 4 eV there are additional shoulders developing into peaks which are strongly affected by quantum confinement effects. In the Ge case, a more or less monotonic shift to lower energies can be found with increasing crystallite size. The peak positions are 4.1, 3.8, and 3.7 eV for the crystallites of 83, 147, and 239 atoms, respectively. This peak might become the E_1 structure in unstrained bulk Ge. For Ge such a shift has been predicted.[8,48] However, the suggested confinement energy overestimates the effect for the crystallites under consideration. The effective-mass approximation is not valid for crystallite radii smaller than 1 nm. In any case, the shifts do not obey a R^{-2} law (R is the crystallite radius). The variation with the radius is weaker.

For the Si crystallites, on the other hand, no simple description of the low-energy shoulders and peaks can be given. In order to understand these features in greater detail we study the influence of the gap states. In Fig. 6 the contribution of the occupied gap states to the absorption spectrum within the optical gap of the host are presented. In order to do this we have restricted the summation over the valence states in expression (1) to a summation over the gap states.

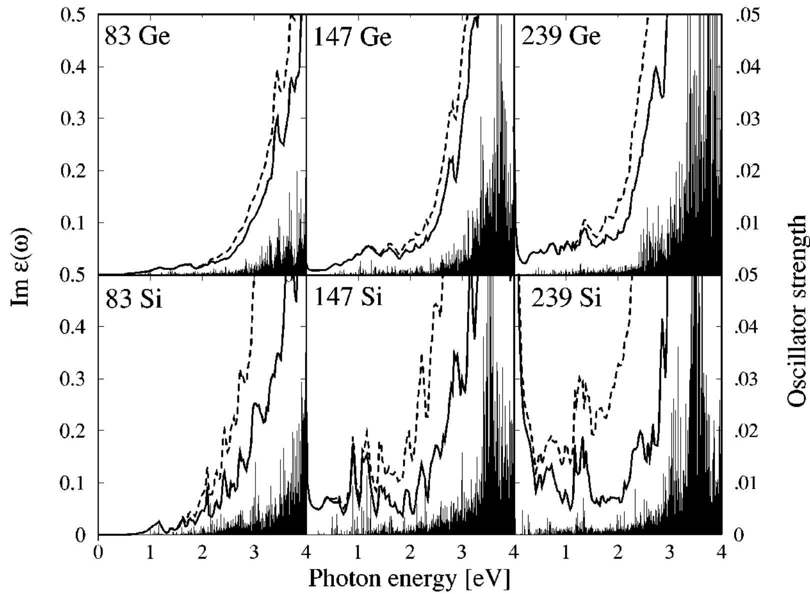

FIG. 6. Contribution of the occupied gap states to the imaginary part of the dielectric function of Ge crystallites with Ge-C crystallite-host interface and of Si nanocrystallites. All crystallites are embedded in cubic SiC in a 512-atom cell. Solid line, gap state contribution; dashed line, imaginary part of the total dielectric function. The oscillator strengths of the contributing optical transitions are indicated by vertical lines.

Below 4.5 eV for Ge and 4 eV for Si nanocrystallites, the spectral properties are determined solely by the gap states. In Fig 6 we have also drawn the oscillator strengths of the transitions against the respective transition energies. For Si the transitions between the highest occupied valence states and the lowest conduction states (cf. Fig. 4) have only very low oscillator strengths. However, they give rise to a structure at a photon energy of about 1 eV. The imaginary part of the dielectric function below 2 eV is at most of the order of 1% of the maximum. Even though the Si crystallites in cubic SiC tend to constitute a type-I system, the transition probabilities of the lowest transitions remain small. This is the reason why the overall dielectric function in Fig. 5 does not strongly reflect the different heterostructure character as compared to Ge. The effect on the luminescence properties might, at this point, only be conjectured at. However, it could be worthwhile to search for an infrared emission after illuminating Si/cubic SiC systems.

The calculation of the real part of the dielectric function (cf. Fig. 5) allows the determination of the electronic dielectric constant of the composite material consisting of Ge or Si nanocrystallites embedded in SiC. Unfortunately, the resulting values cannot be compared directly with experimental values, since local-field effects due to the atomic structure of the matter are not taken into account in our calculations. The values resulting for the bulk materials are generally larger than the macroscopic dielectric constants observed experimentally.[47] For small filling factors, the dielectric constant $\mathrm{Re}\,\varepsilon(0)$ (cf. right panels of Fig. 5) corresponds to the microscopic high-frequency dielectric constant $\varepsilon_\infty = 6.2$ calculated for bulk SiC. With increasing amounts of Ge or Si, this value increases towards the larger Ge dielectric constant. We have calculated $\varepsilon_\infty = 13.7$ and 17.1 for unstrained Si and Ge.

The dielectric constants of the composite materials are plotted in Fig. 7 against the filling factor. With increasing fractions of the crystallite material, the effective gap between occupied and empty states is reduced. This results in larger effective dielectric constants of the electronic system under consideration. However, the increase depends on the interaction of the nanocrystallites, i.e., the supercell size, and the type of interface bonds.

C. Interaction of nanocrystallites

The supercell approach used here gives results for isolated nanocrystallites only in the limit of large supercells and small crystallites. In practice one calculates the electronic and optical properties of an effective medium consisting of an arrangement of nanocrystals in a host material. On the one hand, they depend on the barriers for the electrons and holes between the crystallite and host material. On the other hand, the number of nearest-neighbor nanocrystallites (which is the smallest in the sc case), the size of the supercell, and the diameter of the crystallite determine the strength of the interaction of the crystallites in different supercells. This influ-

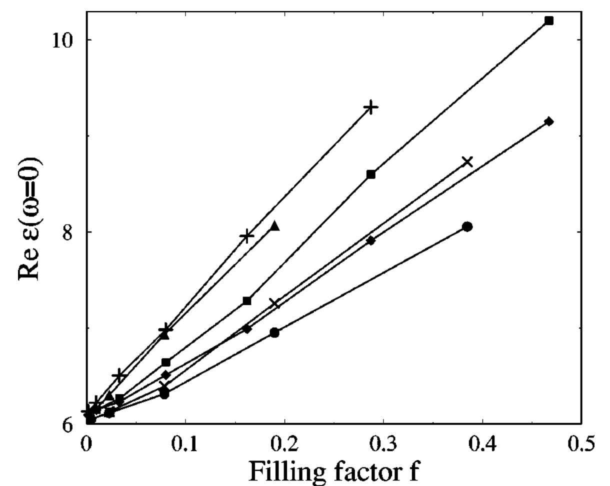

FIG. 7. Dielectric constant of the crystallite-host supercell arrangements. Ge crystallites with Ge-C crystallite-host interface in 216-atom (circle) and 512-atom (diamond) cells, with Ge-Si interface in 216-atom (triangle) and 512-atom cells (plus) as well as Si crystallites in the 216-atom (cross) and 512-atom cells (square).

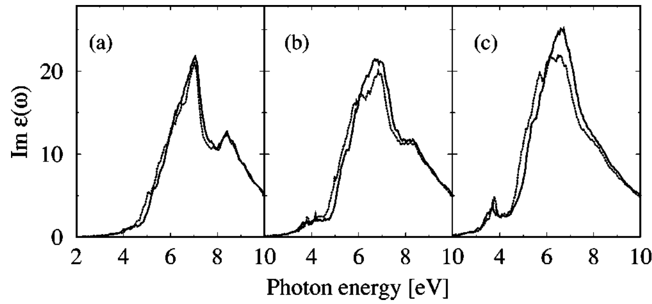

FIG. 8. The imaginary part of the dielectric function of Ge nanocrystals with Ge-Si crystallite-host interface (dotted lines) are compared to Ge nanocrystals with Ge-C crystallite-host interface (solid lines) but with one more shell of Ge atoms. The sizes of the crystallites are 41 (Ge-Si) and 83 (Ge-C) atoms in (a), 83 (Ge-Si) and 147 (Ge-C) atoms in (b), and 147 (Ge-Si) and 239 (Ge-C) atoms in (c).

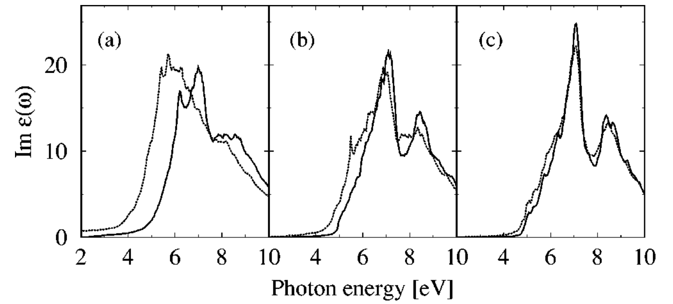

FIG. 9. Imaginary part of the dielectic function of the 17-atom Ge nanocrystal in a (a) 64-atom, (b) 216-atom, and (c) a 512-atom supercell. Solid lines, systems with Ge-C crystallite-host interface, dotted lines, Ge-Si interface.

ences the electronic structure but also includes an electromagnetic coupling, since we calculate a dielectric function of a composite on a nanometer scale.

In order to study these effects we vary the supercell size. In the case of the dielectric constant of the composite system the interaction of the nanocrystallites is already demonstrated in Fig. 7. The increase of the dielectric constant with the filling factor is always weaker for nanocrystallites embedded in 216-atom cells than for those in 512-atom supercells. This is a consequence of the change of the electronic structure. We have also studied the DOS of the 17-atom Ge nanocrystal with a Ge-C interface in different supercells (not shown). The interaction of the nanocrystallites is varied using cells of 512, 216, and 64 atoms. The wave-vector dispersion of the underlying Ge-induced crystallite bands near the VBM of SiC increases with rising strength of the interaction. As a consequence, the peaks in the DOS within the SiC energy gap are broadened. There is a tendency to smear out the fundamental gap of the host. This has already been seen in Figs. 2 and 3 where a stronger dispersion of the crystallite-related states indicates stronger interaction.

D. Influence of nanocrystallite-host interface

Constructing the spherical Ge nanocrystallites shell by shell in the manner described above, we obtain embedded nanocrystallites with only Ge-C or only Ge-Si bonds at the crystallite-host interface. The question arises as to what is to be considered part of the crystallite, and which part of our arrangement belongs to the host material. In the case of Si in SiC only Si-C bonds occur because a spherical crystallite with outer Si-Si bonds is identical to a nanocrystal bounded by Si-C bonds but with one more shell of Si atoms. Therefore we describe the interface effects considering the example of Ge nanocrystallites. Considering the eigenvalues and the covalent radii, Si and Ge atoms are closer in their properties than C and Ge. Therefore, one expects that the first shell of Si after the outermost shell of Ge behaves roughly like one more shell of Ge. In Fig. 8 we illustrate this effect by contrasting the imaginary part of the dielectric function of the Ge nanocrystallite with a Ge-C interface to the respective Ge crystallite with one less Ge shell but with a Ge-Si interface. Evidently there is a close similarity between the respective curves. Differences in the intensities appear mainly in the range of the first main absorption peak of SiC and the Ge-related shoulder at its low-energy side. They become stronger with increasing numbers of interface bonds. The other quantities we have calculated, like the DOS and the band structure, corroborate the interpretation of the outermost Si shell acting roughly like another Ge shell.

The sizes of the considered nanocrystallites are still rather small. For the 41-atom crystallite the number of crystallite-host interface bonds is about the same as the number of intracrystallite bonds. For the smaller crystallites the ratio is even larger. For the largest nanocrystallite of 239 atoms, there are only twice as many intracrystallite bonds as there are interface bonds. These numbers show that a simple picture of a volume crystallite material and interfaces to the host material cannot be completely correct for the systems discussed in this work.

The interplay of interface effects, nanocrystallite interaction, and different filling factors is illustrated in Fig. 9 studying the imaginary part of the dielectric function of the 17-atom Ge nanocrystallite embedded in 64-atom, 216-atom, or 512-atom supercells with both possible interfaces in each case. In the 512-atom supercells the two different interfaces give rise to rather similar spectra. They are determined mostly by the large amount of SiC host material. The results become completely different for small supercells. The differences in the electronic structures due to the different interfaces become more important. Moreover, the different numbers of Si and C atoms of the host material contribute to the differences. The character of the host spectrum is widely perturbed. One has to discuss the properties of a new composite material instead of a nanocrystallite embedded in a matrix material.

IV. SUMMARY

We have developed a first-principles method to calculate the optical properties of nanocrystallites embedded in a crystalline matrix. This method is based on the independent-particle approximation and the supercell approach. Using supersoftened non-norm-conserving pseudopotentials we are able to treat simple-cubic cells of up to 512 atoms fully

quantum mechanically (even including first-row elements). These supercells make it possible to study spherical nanocrystallites of up to 239 atoms, which have been constructed by replacing the host atoms by Ge or Si shell by shell of next neighbors, starting from either a Si or C atom. We applied the density-functional theory and a pseudopotential-plane-wave scheme. The similarities between the non-norm-conserving pseudopotential and the projector-augmented wave schemes have been used to construct all-electron wave functions of the valence electrons and, hence, to calculate optical matrix elements. A recent refinement of the linear tetrahedron method allowed us to restrict the electronic-structure calculations to one **k** point in the Brillouin zone. We have studied Ge and Si nanocrystallites embedded in the wide-band-gap semiconductor cubic SiC, and calculated band structures, the density of states, and the dielectric function.

We found that the properties of the embedded nanocrystallites depend strongly on the crystallite material, the crystallite size, the crystallite interaction, the type of the interface to the host crystal, and the electronic properties of the host. While the embedded Ge nanocrystallites turn out to constitute a type-II heterostructure, the Si crystallites show also features of a type-I system. For Ge nanocrystallites, only the uppermost hole states are localized within the crystallite region. The Si crystallites also induce empty states within the gap of the host material.

The interaction between nanocrystallites in adjacent supercells gives rise to a dispersion of the crystallite-induced energy levels. The band structure and DOS show that via this dispersion the crystallite-induced bands might smear out the fundamental gap of the host. For Ge and Si nanocrystals embedded in cubic SiC with an experimental gap of about 2.4 eV, the quantum confinement only affects the lowest peak in the optical absorption spectrum. This peak is particularly pronounced for Ge. The interface bonds play an important role in the optical spectra because of the smallness of the nanocrystallites considered in this work. It is even difficult to decide which atoms of the system belong to the crystallite. The first shell of Si atoms around a Ge crystallite with a Ge-Si interface behaves very similar to one more shell of Ge.

ACKNOWLEDGMENTS

We acknowledge financial support from the Deutsche Forschungsgemeinschaft (Sonderforschungsbereich 196, Project No. A8) and the European Community within a Training Research Network (Contract No. CT-2000-00167). A part of the numerical calculations has been done using the facilities of the J. v. Neumann Institute for Computing in Jülich.

[1] Y. Maeda, N. Tsukamoto, Y. Yazawa, Y. Kanemitsu, and Y. Masumoto, Appl. Phys. Lett. **59**, 3168 (1991).

[2] S. Schuppler, S.L. Friedman, M.A. Marcus, D.L. Adler, Y.-H. Xie, F.M. Ross, Y.J. Chabal, T.D. Harris, L.E. Brus, W.L. Brown, E.E. Chaban, P.F. Szajowski, S.B. Christman, and P.H. Citrin, Phys. Rev. B **52**, 4910 (1995).

[3] T. van Buuren, L.N. Dinh, L.L. Chase, W.J. Siekhaus, and L.J. Terminello, Phys. Rev. Lett. **80**, 3803 (1998).

[4] M.D. Mason, G.M. Credo, K.D. Weston, and S.K. Buratto, Phys. Rev. Lett. **80**, 5405 (1998).

[5] S. Schieker, O.G. Schmidt, K. Ebert, N.Y. Jin-Phillipp, and F. Phillipp, Appl. Phys. Lett. **72**, 3344 (1998).

[6] C.S. Peng, Q. Huang, W.Q. Cheng, J.M. Zhou, Y.H. Zhang, T.T. Sheng, and C.H. Tung, Phys. Rev. B **57**, 8805 (1998).

[7] S. Takeoka, M. Fujii, S. Hayashi, and K. Yamamoto, Phys. Rev. B **58**, 7921 (1998).

[8] K.L. Teo, S.H. Kwok, P.Y. Yu, and S. Guha, Phys. Rev. B **62**, 1584 (2000).

[9] L. Pavesi, L. Dal Negro, C. Mazzoleni, G. Franzo, and F. Priolo, Nature (London) **408**, 440 (2000).

[10] P. Tognini, L.C. Andreani, M. Geddo, A. Stella, P. Cheyssac, R. Kofman, and A. Migliori, Phys. Rev. B **53**, 6992 (1996).

[11] A. Fissel, K. Pfennighaus, and W. Richter, Appl. Phys. Lett. **71**, 2981 (1997); Thin Solid Films **381**, 88 (1998).

[12] D. Kovalev, H. Heckler, M. Ben-Chorin, G. Polisski, M. Schwartzkopff, and F. Koch, Phys. Rev. Lett. **81**, 2803 (1998).

[13] P.Y. Yu and M. Cardona, *Fundamentals of Semiconductors* (Springer, Berlin, 1995).

[14] C.E. Bottani, C. Mantini, P. Milani, M. Manfredini, A. Stella, P. Tognini, P. Cheyssac, and R. Kofman, Appl. Phys. Lett. **69**, 2409 (1996).

[15] L. Wang and A. Zunger, in *Nanocrystalline Semiconductor Materials*, edited by P.V. Kamat and D. Meisel (Elsevier Science, New York, 1996); J. Phys. Chem. **98**, 2158 (1994).

[16] Nicola A. Hill and K.B. Whaley, Phys. Rev. Lett. **75**, 1130 (1995); J. Electron. Mater. **25**, 269 (1996).

[17] S. Ögüt, J.R. Chelikowsky, and S.G. Louie, Phys. Rev. Lett. **79**, 1770 (1997).

[18] C. Delerue, M. Lannoo, and G. Allan, Phys. Rev. Lett. **84**, 2457 (2000).

[19] R.W. Godby and I.D. White, Phys. Rev. Lett. **80**, 3161 (1998).

[20] A. Franceschetti, L.W. Wang, and A. Zunger, Phys. Rev. Lett. **83**, 1269 (1999).

[21] S. Ögüt, J.R. Chelikowsky, and S.G. Louie, Phys. Rev. Lett. **80**, 3162 (1998); **83**, 1270 (1999).

[22] L.-W. Wang and A. Zunger, Phys. Rev. Lett. **73**, 1039 (1994).

[23] C. Delerue, G. Allen, and M. Lannoo, Phys. Rev. B **48**, 11 024 (1993).

[24] I. Vasiliev, S. Ögüt, and J. Chelikowsky, Phys. Rev. Lett. **86**, 1813 (2001).

[25] Y.M. Niquet, G. Allen, C. Delerue, and M. Lannoo, Appl. Phys. Lett. **77**, 1182 (2000).

[26] M. Palummo, G. Onida, and R. del Sole, Phys. Status Solidi A **175**, 23 (1999).

[27] P. Hohenberg and W. Kohn, Phys. Rev. **136**, B864 (1964).

[28] W. Kohn and L.J. Sham, Phys. Rev. **140**, A1133 (1965).

[29] J.P. Perdew and A. Zunger, Phys. Rev. B **23**, 5048 (1981).

[30] S.G. Louie, S. Froyen, and M.L. Cohen, Phys. Rev. B **26**, 1738 (1982).

[31] D. Vanderbilt, Phys. Rev. B **41**, 7892 (1990).
[32] J. Furthmüller, P. Käckell, F. Bechstedt, and G. Kresse, Phys. Rev. B **61**, 4576 (2000).
[33] G. Kresse and J. Furthmüller, Comput. Mater. Sci. **6**, 15 (1996); Phys. Rev. B **54**, 11 169 (1996).
[34] B. Adolph, V.I. Gavrilenko, K. Tenelsen, F. Bechstedt, and R. Del Sole, Phys. Rev. B **53**, 9797 (1996).
[35] L. Dorigoni, O. Bisi, F. Bernardini, and S. Ossicini, C.M. Bertoni, M. Biagini, A. Lugli, G. Roma, and O. Bisi, Thin Solid Films **297**, 154 (1997).
[36] L. Dorigoni, O. Bisi, F. Bernardini, and S. Ossicini, Phys. Rev. B **53**, 4557 (1996).
[37] M.S. Hybertsen and S.G. Louie, Phys. Rev. B **34**, 5390 (1986).
[38] M. Rohlfing and S.G. Louie, Phys. Rev. Lett. **80**, 3320 (1998).
[39] P.E. Blöchl, Phys. Rev. B **50**, 17 953 (1994).
[40] G. Kresse and D. Joubert, Phys. Rev. B **59**, 1758 (1999).
[41] B. Adolph, J. Furthmüller, and F. Bechstedt, Phys. Rev. B **63**, 125108 (2001).
[42] H. Kageshima and K. Shiraishi, Phys. Rev. B **56**, 14 985 (1997).
[43] H.-Ch. Weissker, J. Furthmüller, and F. Bechstedt, Phys. Rev. B **64**, 035105 (2001).
[44] C.J. Pickard and M.C. Payne, Phys. Rev. B **59**, 4685 (1999).
[45] H.-Ch. Weissker, J. Furthmüller, and F. Bechstedt, Mater. Sci. Forum **353-356**, 413 (2001).
[46] W.A. Harrison, *Electronic Structure and the Properties of Solids* (Dover, New York, 1989).
[47] V.I. Gavrilenko and F. Bechstedt, Phys. Rev. B **55**, 4343 (1997).
[48] C.S. Johnson and L.G. Pedersen, *Problems and Solutions in Quantum Chemistry and Physics* (Dover, New York, 1986), p. 122.